Paper 45

Proceedings of the Eleventh International Conference
on Computational Structures Technology,
B.H.V. Topping, (Editor),
Civil-Comp Press, Stirlingshire, Scotland

Modelling of Piezocomposite Functionally Graded Plates for Active Vibration Control

M. Pietrzakowski
Institute of Machine Design Fundamentals
Warsaw University of Technology, Poland

Abstract

The study presented in this paper develops models of active laminated plates with monolithic piezopolymer sensor layers and composite actuator layers being a functionally graded piezoelectric material (FGPM). The FGPM actuator is considered as a multi-layer structure stacked of distinct piezoelectric fiber composite (PFC) laminae. The laminae differ from each other by the amount of aligned piezoceramic fibres to change the actuator electromechanical properties across the thickness. Two distribution functions, which estimate the gradient of constituents, are applied i.e. power and parabolic. The performance of the FGPM actuators equipped with interdigitated electrodes refers to the poling direction along the fibres. It is assumed that the sensor/actuator layers operate in a closed-loop with velocity feedback. The dynamic analysis is based on the classical laminated plate theory and concerns the transverse vibration suppression of rectangular simply supported symmetrically laminated plates. The numerical simulations are accomplished for recognizing the influence of the applied material compositional gradation on changes in the effective elastic and piezoelectric properties across the FGPM actuators and the active plate structural response presented in terms of amplitude-frequency characteristics. The changes in both the natural frequencies and resonant amplitudes are compared and the influence of the piezoceramic material gradation on the control system operational effectiveness is also discussed.

Keywords: laminated plate, piezoceramic control, functionally graded actuator.

1 Introduction

Piezoelectric materials are being used in a wide variety of technical applications especially in the field of structural vibration control of thin-walled flexible structures. Piezoelectric transducers operating as sensors and actuators are formed as patches or layers, which embedded or surface mounted are integrated with the host structure. A brittle nature of monolithic piezoceramics PZT (lead-zirconate-titanate), typically used for actuation because of their high electromechanical efficiency, makes them vulnerable to accidental breakage as well as cracks caused by the host structure curvature related to the operational loads. One way to overcome this shortage is to use active composites reinforced with piezoceramic fibres. This concept was presented by Bent and Hagood [1] who formulated constitutive equations for piezoelectric fiber composites (PFCs) equipped with interdigitated (ID) electrodes and electrically supplied along the fibres. The modelling of laminated plates consisted of these type piezocomposite active elements was developed in references [2, 3] where the structural vibration control effectiveness has been compared depending on the piezocomposite spatial configuration and the fiber volume fraction.

To achieve satisfactory control effectiveness a relatively large deformation of distributed piezoelectric actuators has to be produced. Thus, the interaction between the piezoelectric element and the host structure creates great interlayer shear stresses, which may cause a damage of the control system by local delamination or/and cracking. A sharp change in elastic properties of bonded monolithic piezoceramic actuators and the host structure material also enhance the shear stress concentration. Hence, using elastic piezocomposite patches or layers, which are able to adapt to the structure curvature and whose electromechanical properties vary smoothly in the thickness direction reducing the interlayer shear stresses, may significantly diminish a risk of the control system failure. Modern piezoelectric materials with arbitrary compositional gradient offer required advantages improving the operational reliability and durability of piezoelectric transducers. Usually, elastic and piezoelectric properties are graded along the thickness of functionally graded piezoelectric materials (FGPMs) by changing the volume fraction of the constituents. The static transverse displacements and stress field in FGPM laminates composed of layers whose electromechanical properties vary from layer to layer is analysed in reference [4]. Design of bimorph piezocomposite functionally graded actuators and the finite element modelling for the static and dynamic analysis can be found in references [5, 6]. The dynamic stability analysis of the FGPM plate under the time-dependent thermal load is presented in reference [7]. The effects of continuous material gradation on the actuator properties and the structural response of the plate are numerically examined by the author in [8, 9] where in [9] some aspects of modelling of multi-layer functionally graded PFC actuators are discussed.

This paper aims to develop the models of active laminated plates with FGPM actuator layers characterized by almost continuous gradation of elastic and piezoelectric properties along their thickness. The considered representation is a multi-layer actuator composed of unidirectional PFC laminae (each of different amount of PZT fibres) stacked that the PZT material volume fraction changes through the thickness of the actuator. Two distribution patterns are considered which are approximated by power and parabolic functions, respectively. The dynamic analysis is based on the classical laminated plate theory (CLPT) and concerns steady-state problem. The active reduction of transverse vibration of the rectangular laminated plate is achieved applying the velocity feedback control. Numerical simulations are performed to recognize the influence of the applied PZT fraction distribution on the gradient of elastic and piezoelectric properties within the FGPM actuators, and the plate structural response presented in terms of amplitude-frequency characteristics. The changes in both the natural frequencies and resonant amplitudes are compared and the influence of the PZT ceramics gradation on the control system operational effectiveness is also numerically investigated.

2 Modelling of the system and formulations

Consider a thin rectangular symmetrically laminated plate composed of classic orthotropic layers (e.g. graphite-epoxy, glass-epoxy) integrated with piezoelectric sensor and actuator layers operating in a closed loop with the constant gain velocity feedback. It is assumed that the PVDF (polyvinylidene fluoride) sensor layers are polarized transversally while the multi-layer FGPM actuators equipped with interdigitated electrodes are polarized along the piezoceramic fibres. To produce the bending mode action the FGPM actuators, whose location and material properties distribution is midplane symmetric, are with either opposite polarization or opposite applied electric field. For example, the laminate geometry with indicated co-ordinates is presented in Figure 1.

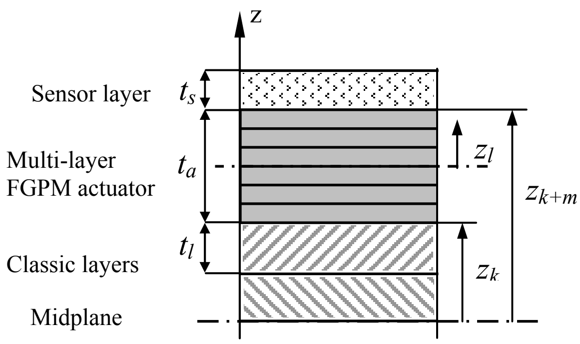

Figure 1: A schematic laminate cross-section with geometry notation

The transverse vibration $w(x,y,t)$ of the active globally orthotropic plate subjected to the external distributed load $q(x,y,t)$ can be determined by the equation

$$D_{11}w_{,xxxx} + 2(D_{12} + 2D_{66})w_{,xxyy} + D_{22}w_{,yyyy} + \tilde{\rho}t_c w_{,tt} = q(x,y,t) - p(x,y,t) \qquad (1)$$

where D_{ij} (i, j = 1, 2, 6) are the elements of the bending stiffness matrix, which are complex for a viscoelastic material, t_c and $\tilde{\rho}$ are the total thickness and equivalent mass density of the plate, respectively, $p(x,y,t)$ is the loading produced by the piezoelectric control system. The subscript comma indicates partial differentiation with respect to the variable after the comma.
The bending stiffness D_{ij} for the n-layered laminate is defined as the following sum of integrals

$$D_{ij} = \sum_{k=1}^{n} \int_{z_{k-1}}^{z_k} \bar{c}_{ij}^{k} z^2 dz \tag{2}$$

where $\bar{c}_{ij}^{k}$ $(i, j = 1, 2, 6)$ are the stiffness coefficients for the kth layer of thickness $t_k = z_k - z_{k-1}$, which are determined with respect to the x, y, and z reference plate axes with the z co-ordinate measured from the midplane in the thickness direction.

The control loading $p(x,y,t)$ is produced by the FGPM actuators driven by the voltage generated in the sensor layers and then transformed according to the control algorithm. Assuming simply supported boundary conditions and applying the closed loop control with velocity feedback the solution to the governing Equation (1) gives the transverse displacement field for the considered active plate. In the case of steady-state vibration the results may be expressed in terms of amplitude-frequency characteristics.

2.1 Relations of the FGPM actuator

The considered actuator is treated as a multi-layer structure consisted of the PFC laminae with PZT fibres arranged according to the rectangular packing pattern and polarized longitudinally. The interdigitated electrodes designed with finger-like sections of alternating polarity are used to direct the electric field along the fibres, thus taking advantage of the d_{33} mode actuation. Modification of the electromechanical properties is obtained by the PZT material volume fraction (number of PZT fibres), which is constant for each lamina and graded through the total thickness t_a of the actuator. As an example of the FGPM actuator the set of distinct PFC laminae with the outer plies equipped with the ID electrodes is shown in Figure 2.

Basing on the periodic unit cell model and applying the uniform field method the effective properties of the two-phase composite material of each PFC lamina are determined. Details of the piezocomposite model and the way of formulation of the effective constitutive relations one can find in references [1, 2].

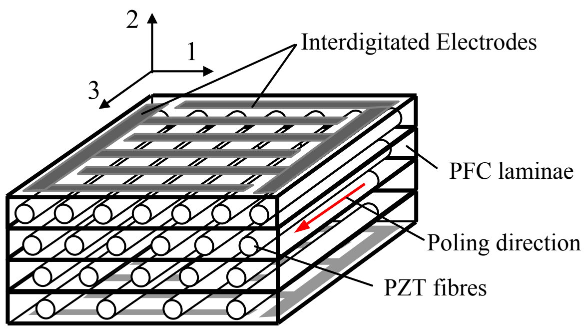

Figure 2: Configuration of the FGPM multi-layer actuator with the ID electrodes

The actuator performance is described by the constitutive equation of the reverse piezoelectric effect. In general, the constitutive equation reduced to the actuation in the 3-1 plane and transformed to the *x*, *y* plate reference axes for each PFC lamina can be written in the form

$$\overline{\boldsymbol{\sigma}} = \overline{\mathbf{c}}^{ef}\,\overline{\boldsymbol{\varepsilon}} - E_3\,\mathbf{R}\,\mathbf{e}^{ef} \tag{3}$$

where $\overline{\boldsymbol{\sigma}} = [\sigma_x, \sigma_y, \tau_{xy}]^T$ and $\overline{\boldsymbol{\varepsilon}} = [\varepsilon_x, \varepsilon_y, \gamma_{xy}]^T$ is the in-plane stress and strain representation, respectively, $\overline{\mathbf{c}}^{ef}$ is the effective stiffness matrix, $\mathbf{e}^{ef} = \left[e_{33}^{ef}, e_{31}^{ef}, 0\right]^T$ is the matrix of the effective piezoelectric stress coefficients referred to the material axes, E_3 is the electric field in the 3-axis direction, **R** is the transformation matrix related to the skew angle between the 1, 3 PFC material axes and the *x*, *y* plate reference axes.

The effective electromechanical properties depend on the PZT volume fraction and the fiber spatial configuration. When the rectangular packing pattern for each lamina is applied (fibres of diameters approximately as thick as the layer are aligned in-plane with a constant distance between them), it may be assumed that the linear fraction of piezoceramic material v_2 measured in the 2-axis direction is constant for a distinct lamina (v_2 = constant). Hence, the linear fraction component v_1 (measured in the 1-axis direction), which differs proportionally to the distance between the fibres, determines the PZT volume fraction V within the lamina ($V = v_1 v_2$).

In the case of the considered multi-layer actuator the effective piezoelectric constants strongly depend on the electrode surroundings, i.e. the electric properties of the matrix material, and also the parameters associated with the ID electrode geometry such as the electrode finger width, electrode finger spacing and distance between the electrode and the PZT fibres. The electric field path length differs for the particular laminae and increases for the lamina located further from the electrode. The actuator cross-section with field lines between the sections of the upper and lower electrodes is shown in Figure 3.

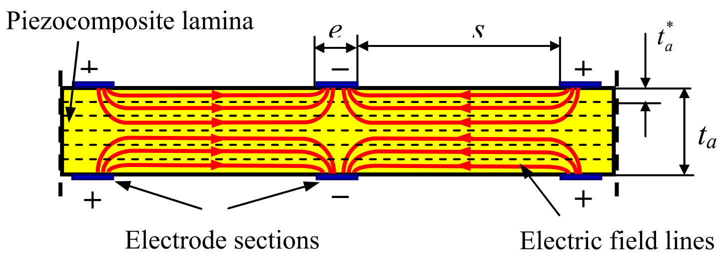

Figure 3: The scheme of ID electrode geometry and electric field lines

For the two-side electroded actuator composed of the laminae of the same thickness t_a^*, the averaged path length within each lamina can be approximated as

$$l_p^{(i)} = (s+e) + (2i-1)(1-v_2)t_a^* \tag{4}$$

where s is the electrode spacing, e is the electrode width, i indicates the lamina number in the sequence from the upper (or lower) electrode to the opposite face, i = 1, 2,…, m, and m denotes the total number of laminae in the FGPM actuator.

For simplification it is assumed that the electric potential function is linear through the total path length between interdigitated electrode sections and the electric field is constant for each actuator lamina.

The FGPM multi-layer actuator is a two-phase composite described by an approximated variation of the volume fraction of piezoceramic and matrix components throughout the thickness. Two patterns are under consideration: the power function and parabolic function. The PZT volume fraction distribution in accordance with a power low can be expressed as

$$v(z_l) = V_{\max}\left[\frac{1}{R} + \left(1-\frac{1}{R}\right)\left(\frac{1}{2} + \frac{z_l}{(m-1)\,t_a^*}\right)^p\right] \tag{5}$$

while in the case of parabolic distribution is given by

$$v(z_l) = V_{\max}\left[1 - \left(1-\frac{1}{R}\right)\left(\frac{2z_l}{(m-1)t_a^*}\right)^2\right] \tag{6}$$

where z_l is the local co-ordinate measured from the middle surface of the actuator, R denotes the inhomogeneity parameter of the FGPM across the thickness for the considered distribution functions, which is defined as the ratio of the maximal to minimal PZT volume fractions, p is the power function exponent.

Assuming that the actuator layers are perfectly integrated with the laminate the actuation transferred from the FGPM actuators to the host structure may be described by the control moment distributed along the edges of the activated area, which mostly coincide with the edges of the actuator layer.

$$\mathbf{M}^E = \left[M_x^E, M_y^E, M_{xy}^E\right]^T \tag{7}$$

In the case when the material axes correspond with the plate axes the analysis concerns a two-dimensional actuation effect. Taking into account the electric term of the constitutive Equation (3) the moment resultant $\mathbf{M}^{\mathrm{E}}$ for the particular FGPM actuator is obtained. For the multi-layer actuator the moment produced can be expressed as

$$\mathbf{M}^E = \sum_{i=1}^{m} \left(\mathbf{e}^{ef}\right)^{(i)} t_a^* z_0^{(i)} E_3^{(i)} \tag{8}$$

where $z_0^{(i)}$ is the distance of the ith lamina from the midplane of the plate, $\left(\mathbf{e}^{ef}\right)^{(i)}$ is the effective piezoelectric constant matrix of the ith lamina, which for the considered material axes orientation refers to the x, y plate axes.

The portion of the electric field $E_3^{(i)}$ supplying the ith component lamina can be expressed due to the electric field-voltage relation. When voltage $V_a(t)$ is applied to the ID electrodes on the both faces of the m-layered actuator the electric field within ith lamina can be approximated by the formula

$$E_3^{(i)} = V_a(t)\left(\frac{1}{l_p^{(i)}} + \frac{1}{l_p^{(m+1-i)}}\right) \tag{9}$$

It is obvious that the electric field becomes smaller with increasing the field path length $l_p^{(i)}$, i.e. when the distance of the lamina from the electrode surface is greater.

The voltage V_a driving the actuator is generated by the PVDF sensor and then transformed due to the velocity feedback control. Finally, the control loading $p(x,y,t)$ produced by the pair of actuator layers located symmetrically about the middle of the plate is

$$p(x,y,t) = 2\left(M^E_{x,xx} + M^E_{y,yy} + 2M^E_{xy,xy}\right) \tag{10}$$

When a zero skew angle between the plate axes and the piezocomposite material axes exists the twisting moment component M^E_{xy} vanishes and bending actuation dominates.

2.2 Relations of the sensor

The sensor equation is formulated based on the constitutive law of direct piezoelectric effect, which for the transversally polarized layer with the in-plane material axes 1, 2 and the 3-axis in the thickness direction, after eliminating the external electric field becomes

$$D_3 = \mathbf{e}^T \boldsymbol{\varepsilon} \tag{11}$$

where D_3 is the electric displacement in the 3-axis direction, $\boldsymbol{\varepsilon}$ is the in-plane sensor strain representation, $\mathbf{e} = [e_{31}, e_{32}, 0]^T$ is the piezoelectric coefficient matrix, which is associated with the strain coefficient matrix $\mathbf{d} = [d_{31}, d_{33}, 0]^T$ according to the relationship $\mathbf{e} = \mathbf{c}\,\mathbf{d}$ with $\mathbf{c}$ – sensor material stiffness matrix.

The voltage produced by the kth sensor layer deformed with the structure is obtained integrating the charge stored on the electrodes. In the study only the flexural strains (bending mode) of the perfectly bonded sensor are considered.

Assuming that the material axes 1, 2, 3 coincide with the plate reference axes x, y, z, respectively, and the electrodes fully cover the sensor faces, after using the standard equation for capacitance, and the geometric relation between strain and plate transverse displacement the following formula is derived

$$V_s^k = -\frac{t_s z_0^k}{\in_{33} A_s} \mathbf{e}^T \int_0^a \int_0^b \left[w_{,xx}, w_{,yy}, 2w_{,xy} \right]^T dxdy \tag{12}$$

where a and b are the plate dimensions, A_s is the sensor effective electrode area, t_s denotes the layer thickness, z_0^k indicates the distance of the kth sensor layer from the laminate midplane, $\in_{33}$ is the sensor material permittivity.

3 Results of calculations

Calculations have been carried out for a simply supported, cross-ply laminated plate of dimensions 400×400×2 mm. The plate consists of classic graphite-epoxy layers of thickness t_l = 0.15 mm, PVDF sensors of thickness t_s = 0.1 mm, and FGPM actuator layers of thickness t_a = 0.6 mm. The layers are stacked according to the symmetric order $[\mathrm{S}/\mathrm{A}/0°/90°]_s$, where the symbols “S” and “A” indicate the sensor and actuator, respectively. The FGPM actuator is treated as being composed of six distinct piezocomposite laminae of the same thickness and having constant effective properties. The amount of PZT fibres in particular lamina is determined according to the applied compositional gradient. The stiffness parameters of the graphite-epoxy composite are assumed as: Y_{11} = 150 GPa, Y_{22} = 9 GPa, G_{12} = 7.1 GPa, and the mass density ρ = 1600 kg/m^3. The material properties of the PVDF sensor are following: Y_s = 2 GPa, ρ_s = 1780 kg/m^3 and piezoelectric strain constants $d_{31} = 2.3 \cdot 10^{-11}$ mV^{-1}, $d_{32} = 3 \cdot 10^{-12}$ mV^{-1}, which relate to the following stress constants $e_{31} = 4.72 \cdot 10^{-2}$ Cm^{-2}, $e_{32} = 1.52 \cdot 10^{-2}$ Cm^{-2}, respectively. The equivalent damping of the plate composite material is modelled due to the Voigt-Kelvin approach assuming the following retardation time values: $\mu_1 = 10^{-6}$ s, $\mu_2 = \mu_{12} = 4 \cdot 10^{-6}$ s for orthotropic graphite-epoxy layers, $\mu_s = 2 \cdot 10^{-6}$ s for PVDF layers and $\mu_m = 8 \cdot 10^{-6}$ s for matrix material of FGPM actuators. The electromechanical properties of components of the piezocomposite actuator are listed in Table 1.

Parameter	ρ kgm^{-3}	c_{11} GPa	c_{12} GPa	c_{13} GPa	c_{33} GPa	G GPa	e_{31} Cm^{-2}	e_{33} Cm^{-2}	$\in_{33}/\in_0$
PZT-5H	7650	127	80.2	84.7	117	36.3	-4.42	15.5	1392
Matrix	1200	8.15	4.01	4.01	8.15	2.33	0	0	11.2

Table 1: Properties of PFC components [1]

The PZT material gradation across the actuator is described by the power function (Equation 5) with electroelastic properties decreasing toward the middle of the plate, and the parabolic function (Equation 6) with the maximal PZT volume fraction $V_{\max}$ occurs in the middle of the actuator layer.

Figures 4a and 4b show the approximated variation of the effective piezoelectric coefficient e_{33}^{ef} in the thickness direction obtained for power (p = 3) and parabolic distributions, respectively. Here, the parameter R is calculated assuming a constant maximal volume fraction of PZT material $V_{\max}$, which is determined by the maximal value of the linear fraction, $v_{1\max}$ = 0.8, measured in-plane across the fibres. It is evident that diagrams of the elastic modulus gradation and the piezoelectric coefficient are similar in shape, respectively.

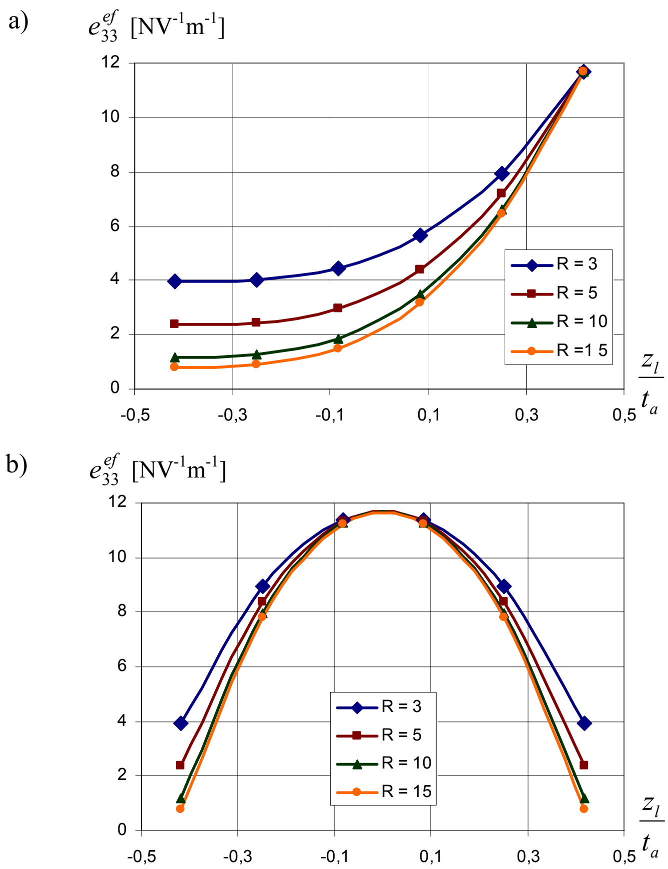

Figure 4: Approximated distributions of the effective piezoelectric coefficient values across the FGPM actuator depending on the parameter R for a) power distribution (p = 3), b) parabolic distribution

The stiffness and mass density, which vary through the FGPM layer thickness, change the natural frequencies of the laminated plate depending on the PZT volume fraction distribution. Figure 5 refers to the power low distribution. Figure 5a shows the influence of the exponent p on the relation between the fundamental frequency ω_{11} and the inhomogeneity parameter R. The natural frequency ω_{11} increases slightly with increasing the power function index ($p > 1$) for greater material inhomogeneity.

The frequency change is noticeable in comparison with the curve obtained for linear distribution (p = 1). The plots of the frequency ω_{11} versus the parameter R are presented in Figure 5b depending on the assumed maximal PZT volume fraction. One can notice that with increasing both the material inhomogeneity and the maximal PZT fraction the frequency ω_{11} becomes greater. The curves increase sharply when the value of R is relatively small with tendency to reduce its increment for larger R.

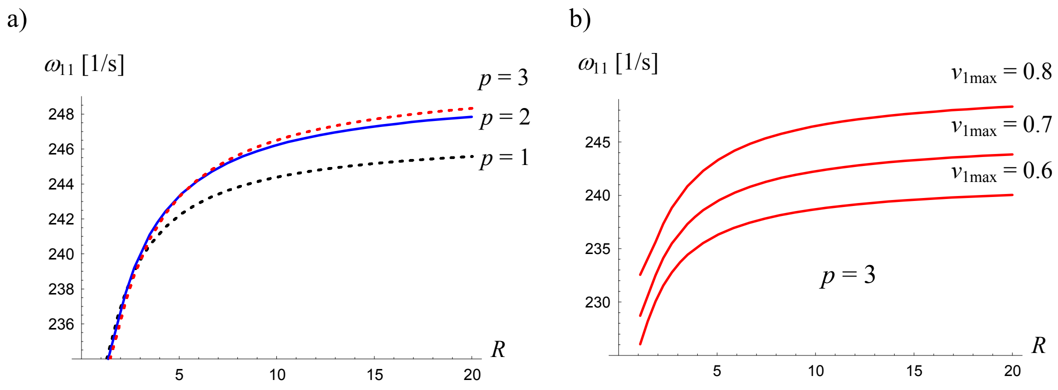

Figure 5: Natural frequency ω_{11} versus the parameter R for the power distribution. a) Influence of the exponent p. b) Influence of the maximal PZT volume fraction

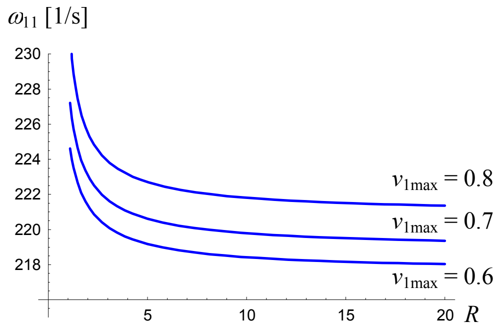

Figure 6: Natural frequency ω_{11} versus the parameter R for the parabolic distribution. Influence of the maximal PZT volume fraction

The analogous diagrams which show the influence of the maximal PZT volume fraction on the natural frequency-material inhomogeneity relation calculated for the parabolic distribution (Equation 6) are presented in Figure 6. Comparing the plots (Figures 5b and 6) it can be seen that the influence of the parameter R on the frequency ω_{11} differs depending on the applied distribution pattern. The plots obtained for the parabolic gradation are decreasing functions starting with a significant slope. But, the compared curves move to higher frequency values with increasing the maximal PZT volume fraction ($v_{1\max}$) for both the power and the parabolic gradations.

To recognize dynamic behaviour of the active plate the amplitude-frequency characteristics depending on the distribution pattern of the applied FGPM actuators are presented in Figures 7 and 8. These characteristics are calculated at the plate point co-ordinates $x = y = 100$ mm for the plate subjected to the uniformly distributed harmonic load of the amplitude $q_0 = 1$ Nm^{-2} and assuming the constant maximal PZT volume fraction determined by $v_{1\max} = 0.8$. The dynamic responses shown in Figures 7a and 7b, which are obtained for the active plate in the vicinity of its first mode frequency, confirm the influence of the particular distribution functions and the parameter R variation on the natural frequency modification. Besides, comparing the plots it can be noticed that with increasing material inhomogeneity of the actuator the resonant amplitudes rise for the multi-layer FGPM actuator types considered. Thus, the operational effectiveness of the control system becomes lower for greater values of the parameter R.

Dynamic responses referred to the power and parabolic FGPM actuators and calculated within a relatively wide frequency range are presented in Figure 8. The parameters of the PZT material distribution are $v_{1\max} = 0.8$ and $R = 10$. For the considered actively damped plate subjected to the uniformly distributed external load the resonance picks are noticeable at the natural frequencies: ω_{11} and ω_{31}. The amplitudes of the higher modes are strongly reduced due to both the active damping and the passive energy dissipation relating to the applied model of material damping.

Comparing the plots it can be seen that the parabolic type actuators offer better control effectiveness shifting the resonance frequencies to lower values. In this case the amplified action is caused by the greater amount of the PZT component in the actuator structure and in consequence improved ability of the control system to generate actuation forces.

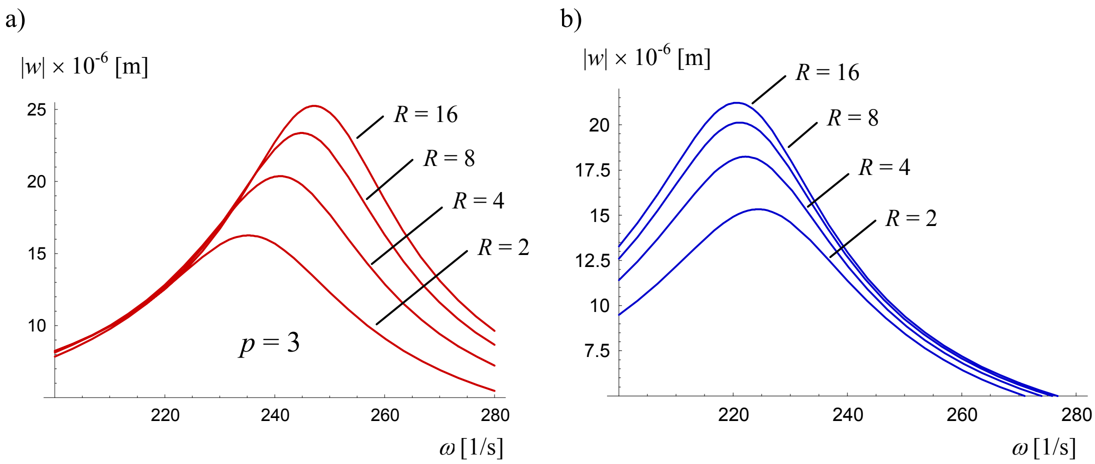

Figure 7: Effects of variations in the parameter R near the first resonance region for a) power distribution, b) parabolic distribution

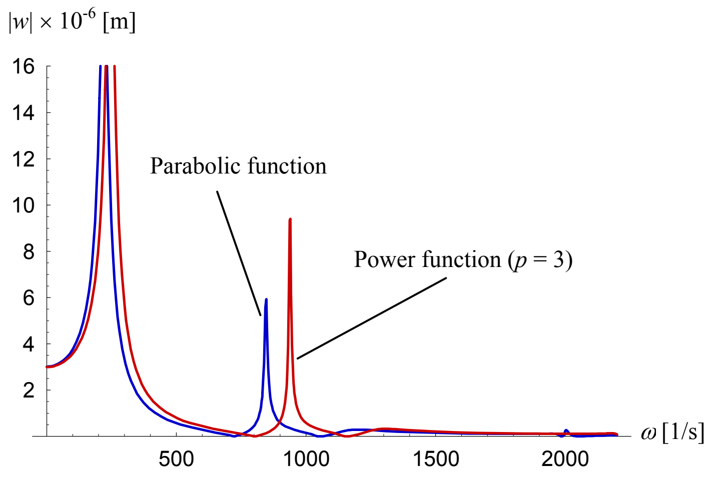

Figure 8: Comparison of the frequency responses of the laminated plate depending on the FGPM gradation

4 Conclusions

The model of the multi-layer FGPM actuator has been formulated as applied to active vibration control of laminated plates. The FGPM actuator concept is based on the almost continuous properties gradation in the thickness direction, which is achieved by stacking the PFC laminae of a different amount of PZT fibres. The effective electromechanical properties of the two-phase composite are obtained due to the uniform field homogenisation method. The theoretical analysis and calculations are performed assuming the actuator material compositional gradient approximated according to the power and parabolic functions. The effects of the PZT fraction distribution on the effective electromechanical properties and the active plate structural response are demonstrated in diagrams. The comparison of changes in both the natural frequencies and the resonant amplitudes depending on the applied gradation patterns and their parameters is discussed. It is observed that for the considered gradations the control system effectiveness becomes lower with increasing the inhomogeneity parameter value and the natural frequencies slightly change. For the same distribution parameters the parabolic type actuators show better control effectiveness because of a greater amount of the PZT fraction.

The results presented proved that the FGPM actuators offer a satisfactory operational effectiveness. Thus, the FGPM actuator layers produce sufficient control forces and by applying a suitable material properties distribution realized during fabrication may also reduce interlayer stresses decreasing significantly a damage hazard in comparison with traditional piezoelectric actuators.

References

[1] A.A. Bent, N.W. Hagood, "Piezoelectric fiber composites with interdigitated electrodes", Journal of Intelligent Material Systems and Structures, 8, 903-919, 1997.

[2] M. Pietrzakowski, "Composites with piezoceramic fibers and interdigitated electrodes in vibration control", Mechanics Quarterly AGH, 22(3), 375-380, 2003.

[3] M. Pietrzakowski, A. Tylikowski, "Effects of piezoelectric fiber arrangement in active laminated structures", Proceedings of AMAS Workshop on Smart Materials and Structures, SMART'03 (eds. J. Holnicki-Szulc, P. Kołakowski), 159-168, 2004.

[4] A. Almajid, M. Taya, S. Hudnut, "Analysis of out-of-plane displacement and stress field in a piezocomposite plate with functionally graded microstructure", International Journal of Solids and Structures, 38, 3377-3391, 2001.

[5] M. Taya, A. Almajid, M. Dunn, H. Takahashi, "Design of bimorph piezo-composite actuators with functionally graded microstructure", Sensors Actuators A 107, 248-260, 2003.

[6] S.Y. Wang, "A finite element model for the static and dynamic analysis of a piezoelectric bimorph", International Journal of Solids and Structures, 41, 4075-4096, 2004.

[7] A. Tylikowski, "Stability of functionally graded plate under in-plane time-dependent compression", Mechanics and Mechanical Engineering, Vol. 7 (2), 5-12, 2004.

[8] M. Pietrzakowski, "Vibration control of functionally graded piezoelectric plates", Mechanics Quarterly AGH, 26 (4), 187-192, 2007.

[9] M. Pietrzakowski, "On functionally graded piezoelectric actuators for applications in structural vibration control", Machine Dynamics Problems, Vol. 32 (4), 78-94, 2008.